Ecological Applications, 0(0), 2017, pp. 1–15

Fragmentation increases wind disturbance impacts on forest structure and carbon stocks in a western Amazonian landscape

Naomi B. Schwartz,[1,6] María Uriarte,[1] Ruth DeFries,[1] Kristopher M. Bedka,[2] Katia Fernandes,[3,4] Victor Gutiérrez-Vélez,[5] and Miguel A. Pinedo-Vasquez[3,4]

[1]*Department of Ecology, Evolution, and Environmental Biology, Columbia University, New York, New York 10027 USA*
[2]*NASA Langley Research Center, Hampton, Virginia 23681 USA*
[3]*International Research Institute for Climate and Society, Columbia University, Palisades, New York 10964 USA*
[4]*Center for International Forestry Research, Bogor 16115 Indonesia*
[5]*Department of Geography and Urban Studies, Temple University, Philadelphia, Pennsylvania 19122 USA*

Abstract. Tropical second-growth forests could help mitigate climate change, but the degree to which their carbon potential is achieved will depend on exposure to disturbance. Wind disturbance is common in tropical forests, shaping structure, composition, and function, and influencing successional trajectories. However, little is known about the impacts of extreme winds on second-growth forests in fragmented landscapes, though these ecosystems are often located in mosaics of forest, pasture, cropland, and other land cover types. Indirect evidence suggests that fragmentation increases risk of wind damage in tropical forests, but no studies have found such impacts following severe storms. In this study, we ask whether fragmentation and forest type (old vs. second growth) were associated with variation in wind damage after a severe convective storm in a fragmented production landscape in western Amazonia. We applied linear spectral unmixing to Landsat 8 imagery from before and after the storm, and combined it with field observations of damage to map wind effects on forest structure and biomass. We also used Landsat 8 imagery to map land cover with the goals of identifying old- and second-growth forest and characterizing fragmentation. We used these data to assess variation in wind disturbance across 95,596 ha of forest, distributed over 6,110 patches. We find that fragmentation is significantly associated with wind damage, with damage severity higher at forest edges and in edgier, more isolated patches. Damage was also more severe in old-growth than in second-growth forests, but this effect was weaker than that of fragmentation. These results illustrate the importance of considering landscape context in planning tropical forest restoration and natural regeneration projects. Assessments of long-term carbon sequestration potential need to consider spatial variation in disturbance exposure. Where risk of extreme winds is high, minimizing fragmentation and isolation could increase carbon sequestration potential.

Key words: Amazon; carbon; forest fragmentation; reforestation; remote sensing; second-growth forest; tropical forest; wind disturbance.

Introduction

Tropical second-growth forests, defined here as forests growing on previously cleared land, can recover biomass quickly and sequester large amounts of carbon (Poorter et al. 2016). These forests could play an important role in mitigating climate change; for example, if allowed to grow undisturbed, existing Latin American second-growth forests could accumulate an additional 8.48 Pg C in the next 40 yr, enough to offset all carbon emissions from fossil fuel use and industrial processes in Latin America and the Caribbean from 1993 to 2014 (Chazdon et al. 2016). Many factors, including past land use, climate, and soil characteristics influence rates and quantities of carbon sequestration in second-growth forests (Anderson-Teixeira et al. 2013, Poorter et al. 2016, Jakovac et al. 2016, Uriarte et al. 2016). In particular, exposure to natural disturbances such as extreme winds, fires, or drought can affect successional trajectories in regenerating forests (Flynn et al. 2009, Uriarte et al. 2009, Anderson-Teixeira et al. 2013, Uriarte et al. 2016), influencing the degree to which the carbon sequestration potential of second-growth forests is achieved. Furthermore, second-growth forests are typically located in landscapes subject to human influence that are mosaics of old growth, second growth, and other land cover types (Brown and Lugo 1990). Regrowth often happens along existing forest margins (Asner et al. 2009, Sloan et al. 2015), making second-growth forests highly exposed to edge effects, impacts of fragmentation, and anthropogenic disturbances such as fire and logging. Accurately predicting biomass recovery in these forests requires that we understand their disturbance ecology

Manuscript received 2 September 2016; revised 1 April 2017; accepted 27 April 2017. Corresponding Editor: Xiangming Xiao.
[6] E-mail: nbs2127@columbia.edu

and how their disturbance regimes are influenced by the landscapes in which they are situated.

Wind is a major disturbance in the tropics and has both short-term impacts and lasting legacies in tropical forests (Everham and Brokaw 1996, Laurance and Curran 2008, Lugo 2008). Tropical forests are exposed to extreme winds from tropical storms or via convective downdrafts, squall lines, and isolated cold fronts. Convective downdrafts and squall lines are relatively common in the Amazon basin (Garstang et al. 1994, 1998), and associated extreme winds can cause large-scale forest disturbance and tree mortality (Espírito-Santo et al. 2010, Negrón-Juárez et al. 2010). Tropical storms and heavy precipitation events are expected to become more intense with climate change (Knutson et al. 2010, Orlowsky and Seneviratne 2012, IPCC 2013), and warming and land use change will affect future convection patterns (Del Genio et al. 2007, Ramos da Silva et al. 2008). Understanding the determinants of forest susceptibility to extreme winds is thus important for modeling and monitoring future impacts of forest disturbance (U.S. Department of Energy 2012).

The spatial distribution and size of blowdowns have important consequences for understanding biomass dynamics in tropical forests (Fisher et al. 2008, Chambers et al. 2009, Di Vittorio et al. 2014, Marra et al. 2016). A number of studies have quantified the frequency, return interval, rotation period, and carbon impacts of large blowdowns in the Amazon across expanses of old-growth forest (Nelson et al. 1994, Negrón-Juárez et al. 2010, Chambers et al. 2013, Espírito-Santo et al. 2014). However, little is known about the impacts of extreme winds in the fragmented, mosaic landscapes in which tropical second-growth forests occur. If forest fragmentation increases the impacts of wind disturbance, this difference could affect estimates of potential carbon sequestration in tropical second-growth forest.

Impacts of extreme wind on both individual trees and stand-level carbon balance differ depending on species composition and forest structure. Damage is most severe for pioneer species, species with low wood density, taller trees, and trees with higher slenderness coefficient, i.e., a larger height for a given diameter (Putz et al. 1983, Zimmerman et al. 1994, Everham and Brokaw 1996, Curran et al. 2008, Canham et al. 2010, Mitchell 2012, Uriarte et al. 2012, McGroddy et al. 2013, Rifai et al. 2016, Ribeiro et al. 2016). Stand structure characteristics such as canopy height, canopy density, basal area, and median diameter are positively correlated with the amount of wind damage in a stand (Everham and Brokaw 1996, Uriarte et al. 2004, McGroddy et al. 2013). Susceptibility to damage also increases with stand age in earlier stages of succession, but may decline in older stands (Everham and Brokaw 1996). These shifts are due to both changes in forest structure and changes in species composition: though canopy height, density, and basal area increase over succession, species composition often shifts away from low-wood-density pioneers toward late-successional species with higher wood density (Bazzaz and Pickett 1980, Lohbeck et al. 2013).

Though second-growth forests are often highly fragmented and located in mosaic landscapes, few studies have considered the influence of landscape and patch structure on wind damage. Fragmentation may influence exposure to strong winds because landscape variability influences the way wind moves, and generates heterogeneity in wind speeds and wind exposure through a number of mechanisms. Wind speeds vary with surface roughness, with winds gaining more speed over low-roughness vegetation such as open grassland, brush, or agricultural crops (Fons 1940, Oliver 1971, Davies-Colley et al. 2000). Accordingly, wind speeds decline with distance from forest–pasture edges (Davies-Colley et al. 2000), and there is strong wind turbulence at high-contrast forest edges (Somerville 1980, Morse et al. 2002, Quine and Gardiner 2007). Wind also moves more quickly though open forest (Somerville 1980, Kanowski et al. 2008). Forest edges have lower biomass and a more open canopy (de Casaneve et al. 1995, Laurance et al. 1997, Harper et al. 2005), implying that wind speeds should be higher at forest edges than in the interior. Furthermore, pioneer species are more common close to forest edges, elevating the vulnerability of edge forest to windthrow (Oosterhoorn and Kappelle 2000, Laurance et al. 2006).

Despite variation in exposure and vulnerability to extreme winds, evidence for impacts of fragmentation on wind damage in tropical forests is lacking. Several studies in temperate silvicultural systems have detected edge effects on wind damage (Peltola 1996, Talkkari et al. 2000, Zeng et al. 2004) but this effect has been more challenging to detect in diverse tropical forests. The Biological Dynamics of Forest Fragments experiment in the Brazilian Amazon found high tree mortality close to forest edges, with uprooting more frequent relative to standing dead trees (Ferreira and Laurance 1997, Laurance et al. 1997, Mesquita et al. 1999). However, this mortality was not linked to specific extreme wind events and could have resulted from other factors (e.g., desiccation). Several studies have examined fragmentation effects on wind damage after tropical storms, and have found little evidence that damage varies with fragmentation (Catterall et al. 2008, Grimbacher et al. 2008). The degree to which fragmentation increases the risk of damage from extreme winds in tropical forests thus remains an open question.

Detecting effects of fragmentation on wind damage may be difficult with a field sampling approach. Extreme winds can be highly patchy (Bellingham et al. 1992, Imbert et al. 1996, Grove et al. 2000, Pohlman et al. 2008). Detecting spatial patterns within heterogeneous, patchy phenomena requires large sample sizes, and inadequate sampling can make it difficult or impossible to detect patterns (Loehle 1991). Estimates of landscape level mortality based on field plot observations may miss up to 17% of mortality (Chambers et al. 2013), and field plot studies may lack the statistical power to detect the effect of fragmentation on wind damage (Grimbacher et al. 2008). However, remote sensing allows detection of patterns that may be unfeasible or impossible in ground-based studies (Chambers et al. 2007). Recently developed remote sensing techniques can detect small blowdowns (Negrón-Juárez et al. 2011). Unlike plot-based approaches, remote sensing allows estimation of wind damage across broad areas, and in combination with field data can improve our understanding of disturbance and carbon dynamics in tropical mosaic landscapes.

Here, we use remotely sensed data to quantify damage from a mesoscale convective storm system across a fragmented production landscape in the Peruvian Amazon. We use these data in combination with land cover maps to ask the following questions: (1) Are second-growth forests more severely fragmented than old-growth forests? (2) How does fragmentation influence forest vulnerability to extreme winds? (3) Does wind damage severity vary in old-growth vs. second-growth forests?

We predict that second-growth forests in our study area will be more severely fragmented than old-growth forests, and hypothesize that severity of wind damage will be highest in small, isolated forest fragments and close to forest edges. We expect that second-growth forests, which have a higher proportion of pioneer species with low wood density, will suffer more severe damage than old-growth forests, composed of less vulnerable high wood density species. This variability could affect forest succession in dynamic, fragmented landscapes, with forest patch and landscape characteristics influencing rates of biomass recovery via effects on exposure and vulnerability to wind disturbance.

Methods

Study area

The city of Pucallpa, the capital of the Ucayali region of Peru, is the largest Amazonian city connected to the national capital, Lima, by road. As a result, Pucallpa is an important transport center, and in recent years has been a hotspot of forest disturbance, deforestation, and fire in the Peruvian Amazon (Oliveira et al. 2007, Uriarte et al. 2012, Schwartz et al. 2015). This research focuses on an area of 2,158 km^2 near Pucallpa, surrounding the highway from Lima to Pucallpa. The landscape is heterogeneous, with patches of old-growth and second-growth forest surrounded by pastures, oil palm plantations, and smallholder farms (Gutierrez-Velez and DeFries 2013; Fig. 1). Elevation ranges from 150 to 250 m above sea level and total annual precipitation

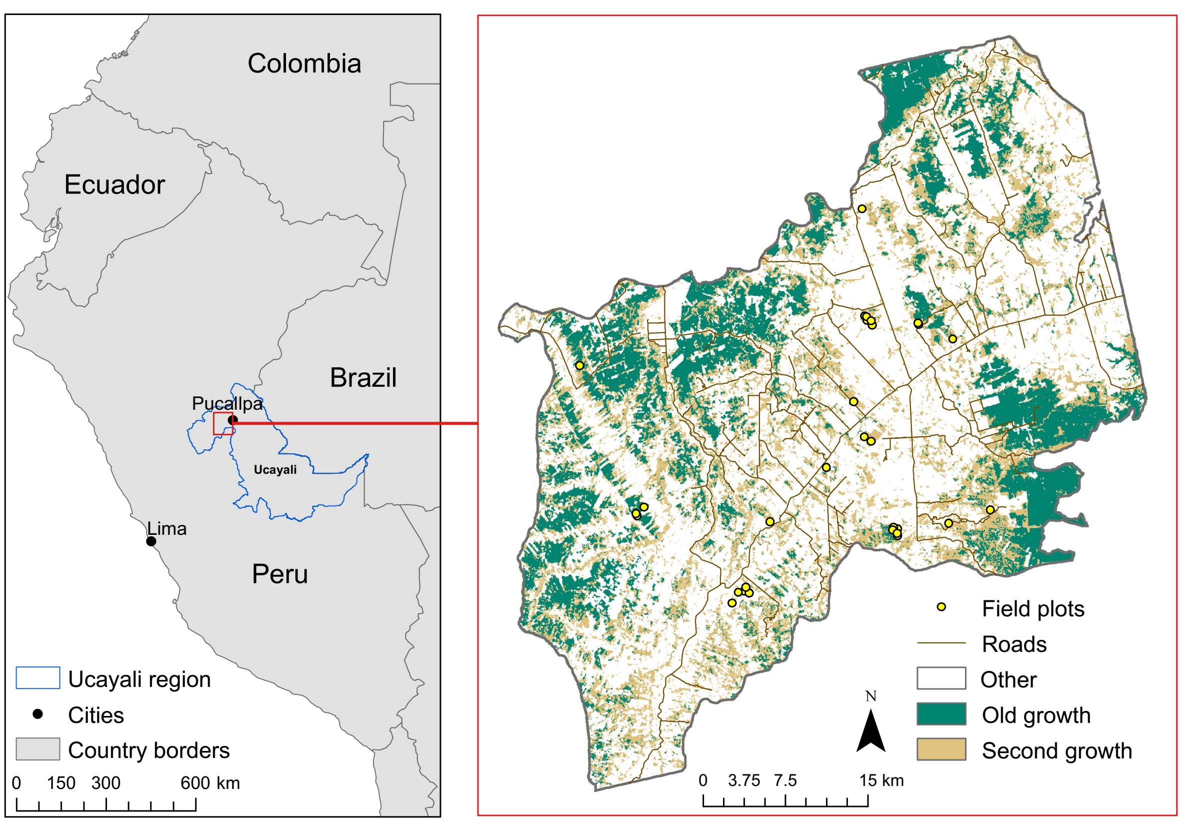

Fig. 1. Location of the study area, near Pucallpa, Ucayali, Peru. Inset depicts forest cover, and locations of field plots and roads.

ranges from about 1,500 to 2,500 mm, with a dry season from July to September.

On 30 November 2013, a mesoscale convective system (MCS) passed through the study area, resulting in widespread blowdowns and tree mortality. Though there is insufficient meteorological station data available from the study area to characterize the storm severity, data processed from the GOES-13 satellite using the method described in Bedka and Khlopenkov (2016) indicates high overshooting top probability during the November 30 storm in the study area (Appendix: Fig. S1). Overshooting tops indicate regions where strong updrafts were present within the MCS. Strong downdrafts are often present near to these updrafts in regions of heavy precipitation. Storms with overshooting tops often generate winds that exceed 58 mph, the criterion for "damaging wind" by the U.S. NOAA National Weather Service (Dworak et al. 2012). Given the heterogeneity in land cover, forest age, and patch size, this landscape offers an ideal opportunity to study how impacts of damaging winds vary with fragmentation and landscape context.

Remote sensing of wind damage

We obtained Landsat 8 OLI scenes covering the study area (path-row 06-066 and 07-066) from 2013 (pre-storm) and 2014 (post-storm; Appendix: Table S1) at 30-m resolution. All scenes were acquired with atmospheric corrections from the Landsat CDR archive (LaSRC product; USGS 2016) via USGS Earth Explorer (*available online*).[7] The LaSRC product includes a cloud mask band, generated with the FMASK algorithm (Zhu and Woodcock 2012). We used this band to mask pixels that were cloudy in 2013 or 2014. An area of 1,023 ha was masked out due to cloud cover, equal to 0.5% of the study area. Because the atmospheric composition between multi-temporal images differs, especially regarding water vapor and ozone, we applying a radiometric normalization (Hall et al. 1991) to normalize the 2014 scene to the 2013 scene, using the MAD algorithm (Canty and Nielsen 2008). All remote sensing data processing was conducted in ENVI (Exelis Visual Information Solutions, Boulder, Colorado, USA) unless otherwise indicated.

To map wind damage, we follow the approach outlined by Negron-Juarez et al. (2010, 2011), which uses spectral mixture analysis (SMA) to map the change in non-photosynthetic vegetation (NPV) fraction across pixels. SMA assumes that every pixel is a linear combination of some number of target endmember spectra, such as vegetation, shade, NPV, and/or bare soil, and quantifies the per-pixel fraction of each endmember (Adams and Gillespie 2006). Wind damage increases the amount of wood, dead vegetation, and litter exposed to the sensor, and so the change in NPV fraction is associated with the amount of wind damage.

[7] http://earthexplorer.usgs.gov/

We applied linear spectral unmixing to each image using endmembers for green vegetation (GV), NPV, and shade. Endmembers were identified from the 2013 scene using the Pixel Purity Index algorithm (Boardman et al. 1995) available in ENVI (Appendix: Fig. S2). Following unmixing, we normalized the fraction of NPV without shade as NPV/(GV + NPV) so that fractions reflected only relative proportions of NPV and GV, and not differences due to effects of shading (Adams and Gillespie 2006). Change in NPV (ΔNPV) was calculated by subtracting the normalized NPV fraction in 2013 from 2014.

Field data collection

Wind damage was measured in the field to assess whether ΔNPV provided an adequate approximation of damage. Because previous studies (Negrón-Juárez et al. 2011, Rifai et al. 2016) had validated the relationship between ΔNPV and wind damage in old-growth forests, we focused our validation and field data collection on second-growth forest. During the months of July and August of 2014 and 2015, we established 30–0.1 ha forest plots (Fig. 1). We used satellite images to identify forest patches, and from those, chose sites where we could locate and get permission from the landowners to access their property. Within these areas, plot locations were selected to encompass a range of ΔNPV. Because plots were slightly larger than a Landsat pixel, plot-level ΔNPV was calculated as the weighted mean of ΔNPV in pixels overlapped by the plot. We determined age of the forest plots from a 28-yr land cover time series (Schwartz et al., *in press*), as the number of years since the last year that the plot location was classified as non-forest. Though all forest plots were located within forest classified as second growth (see *Remote sensing of land cover*), not all had been observed as having been clear-cut during the 30-yr satellite record, and plot ages ranged from 3 yr to >30 (i.e., never cleared). Plots were geolocated using a Garmin GPSMAP 62sc.

In each plot, we measured diameter at breast height (dbh) of all trees >5 cm, and coded each tree as damaged (uprooted, trunk snapped, or severe branch loss) or undamaged. Downed or damaged trees that were severely rotted were marked as such, since these trees were likely damaged prior to the 2013 storm. We conducted all analyses including and excluding these previously damaged individuals and it did not significantly affect our results; reported results exclude these trees. Measures of damage include both stems directly thrown by wind and trees that were damaged by other trees, because it is difficult to distinguish between these two types of damage in the field. We calculated aboveground biomass (AGB) using the following allometric equation developed for secondary forest species in the central Amazon (Nelson et al. 1999):

$$\ln(\text{biomass}) = -1.9968 + 2.4128 \times \ln(\text{DBH}).$$

We divided biomass by two so that estimates were in terms of kg C instead of kg biomass, under the assumption that C makes up 50% of biomass (Brown and Lugo 1982). To characterize plot-level damage, we calculated total damaged biomass, proportion biomass damaged, total stems damaged, and proportion of stems damaged for each plot. We assessed the relationship between ΔNPV and wind damage by calculating linear regressions of ΔNPV vs. field measurements of wind damage in the 30 forest plots. To estimate AGB loss across the study area, we used the parameters from the linear model of ΔNPV vs. total AGB lost in field plots (Appendix: Fig. S6c), and applied it to each forest pixel to calculate lost biomass based on a pixel's NPV. Because allometries based on secondary forest species yield lower estimates of biomass, using an allometric equation designed for secondary forest species across the whole study area is likely to underestimate biomass lost in old-growth forest. Furthermore, wind damage tends to increase with age (Fig. 2), so it is likely that old-growth forests experienced more severe damage than second-growth forests. However, because we measured wind damage in second-growth forests only, we are extrapolating using parameters derived from the relationship between damage and AGB in second-growth forests. Therefore, our estimates represent a conservative estimate of biomass lost across in the study area's forests, particularly for old-growth forests.

Remote sensing of land cover

We developed a land cover classification at 30-m resolution for use in generating predictor variables related to fragmentation and masking analyses to forested areas. The classification expanded on the approach laid out in Gutiérrez-Vélez and DeFries (2013). Land use classes were old-growth forest, second-growth forest, mature oil palm (>3 yr old), and "other," which included young oil palm (<3 yr old), bare ground, burned non-forest areas, fallow, pasture, degraded pasture, and bodies of water. Training data were collected in the field, and for the training data, second-growth forests were identified as tree-dominated vegetation growing in areas that had previously been cleared, with significantly lower basal area than old-growth forests in the study area (Gutiérrez-Vélez et al. 2011). Old-growth forests were identified as predominantly residual forest from logging and extraction of non-timber resources, but they have significantly higher basal area and biomass than second-growth forests (Gutiérrez-Vélez et al. 2011). Ultimately, whether a pixel was classified as old growth or second growth depends on its spectral properties, which do not always coincide with its land-use history.

We classified Landsat 8 OLI images (Appendix: Table S1) with a random forest classification built with several spectral indices and spectral transformations: (1) NDVI; (2) bare soil, vegetation, and shade fractions from SMA; (3) brightness, greenness, and third from a tasseled-cap transformation; and (4) first- and second-order texture measures. Components 1–3 were shown to be effective for classifying the non-oil palm land cover classes in a land cover classification from the same study area (Gutiérrez-Vélez and DeFries 2013). Component 4, the texture measures, were useful for distinguishing oil palm plantations, which are spectrally similar to secondary forests but appear more uniform in satellite images due to even-aged planting. Training and testing data for land cover classes were collected during a 2015 field campaign and included 2,198.52 ha total, divided among classes (Appendix: Table S2). For more details about the classification, see Appendix S1.

The land cover map from 2014 was used to mask analyses to forested areas (old growth and second growth). We also masked areas near known anthropogenic disturbance, since spillover disturbance from recent forest clearing might bias results along forest edges. To do so, we identified recently deforested areas, areas that were classified as forest in 2013 and as non-forest in 2014, and masked all pixels within 60 m to prevent anthropogenic disturbance biasing results (Appendix: Fig. S3).

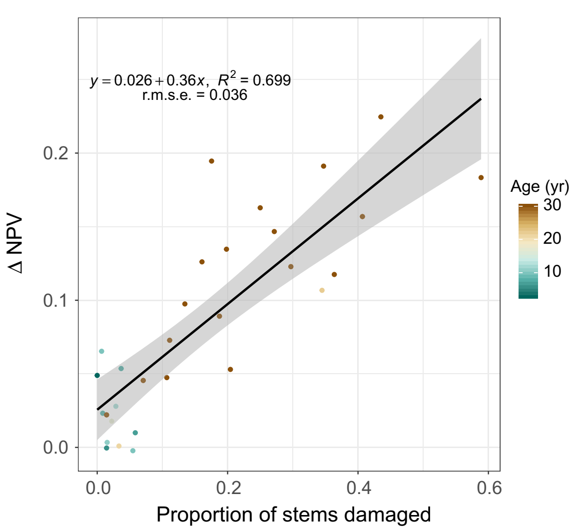

Fig. 2. Change in non-photosynthetic vegetation (ΔNPV) vs. proportion of stems > 5 cm DBH damaged in second growth forest field plots. Shaded areas indicate 95% confidence interval of regression line; r.m.s.e., root mean square error. Regression $P < 0.001$.

Characterizing forest fragmentation

We used Fragstats (McGarigal et al. 2012) to characterize forest patch fragmentation. Old-growth and second-growth forests were all treated as a single forest category for the purpose of characterizing patches. Fragmentation has three key axes: area, edge, and isolation (Fahrig 2003, Haddad et al. 2015). We calculated one Fragstats metric to represent each of these axes (Fig. 3). Patch area (ha) represents patch size. Edginess is quantified with the shape index, which is calculated as

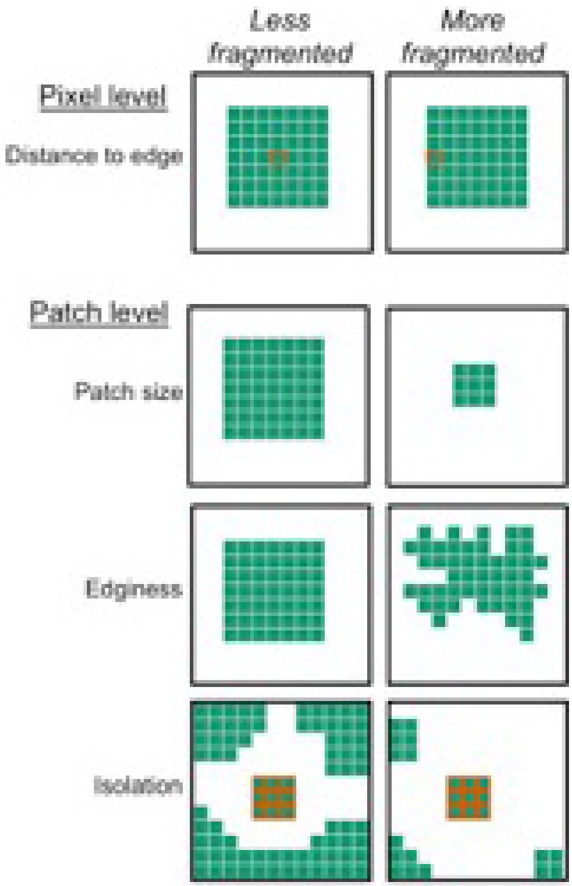

FIG. 3. Conceptual figure illustrating axes of fragmentation and variables associated with fragmentation included in analyses. Green squares represent forest pixels and adjacent pixels represent a patch. Orange outline indicates focal pixel/patch for distance to edge and isolation measures.

$$\mathrm{SHAPE} = \frac{0.25p}{\sqrt{a}}$$

where p is the patch perimeter and a is the patch area. Shape index increases as the perimeter of a patch gets more complex, and equals 1 if a patch is a perfect square. We quantified isolation with the proximity index. The proximity index takes into account the area and distance of forest within a particular radius around the focal patch, and increases from zero with the upper limit determined by the search radius. For a given patch I, proximity index is calculated as

$$\mathrm{PROX} = \sum_{j=1}^{n} \frac{a_{ij}}{h_{ij}^2}$$

where a_{ij} is the area (m^2) of patches $j = 1\ldots n$ within specified neighborhood radius (m) of focal patch i and h_{ij} is the distance (m) between patch i and patch j. Using this formulation assumes that larger and closer patches decrease patch isolation more than smaller or more distant ones, a reasonable assumption. We calculated proximity index with several radii (250, 500, 1,000, 2,000, 4,000, and 10,000 m), but these indices were highly correlated and there was no significant different in model performance depending on the distance, so we used the 1,000 m radius in our final models. So that higher values represented increasing isolation, we multiplied proximity index by −1.

Statistical analysis

We compared sizes of damaged vs. undamaged trees, and fragmentation variables in old- vs. second-growth forest using t tests. To test the relationship between wind damage, forest fragmentation, and forest age (old vs. second growth), we fit a generalized linear model to predict ΔNPV at the pixel scale (Table 1). Pixels with ΔNPV < 0 were excluded from analysis, because a decline in NPV cannot represent negative damage and instead likely represents changes due to forest succession or recovery from prior disturbance. Both pixel characteristics and patch characteristics were included as predictors. Pixel level predictors were distance from forest edge and a binary predictor for second-growth forest (0, old growth; 1, second growth). Patch level predictors were area, edginess, and isolation of the patches in which pixels were located. Because the total number of pixels was large (461,610) and ΔNPV was highly left skewed, we stratified pixels according to ΔNPV (0–0.05, 0.05–0.15, 0.15–0.25, >0.25) and randomly sampled 2,000 pixels from each stratum for use in statistical analyses (Appendix: Fig. S4). The sample was bootstrapped 200 times. ΔNPV was log-transformed to meet the assumption of normality. Distance from edge was also log-transformed because it was highly left-skewed. To facilitate interpretation, all predictors were scaled to unit standard deviation by subtracting the mean and dividing by the standard deviation (Gelman and Hill 2007). To test for collinearity among predictors we calculated variance inflation factors (VIF; Fox and Monette 1992) and condition indices (Belsley 1991). VIF values greater than ~5 indicate strong collinearity (Dormann et al. 2012), though values as low as 2 can have impacts on parameter estimates (Graham 2003). VIF for all predictors was <4 with the exception of edginess (VIF = 5.2). To address this potential collinearity issue, we ran the model with all predictors other than patch area, which was correlated with the other fragmentation predictors and was the predictor with the weakest effect in the full model. The maximum VIF in this partial model was 2.2, and the parameters for all remaining predictors were qualitatively the same as in the full model. We followed the same steps, removing edginess, which had the highest VIF at 2.2. In this partial model, the maximum VIF was 1.4 and still, parameters were qualitatively the same. Condition indices >30 indicate substantial collinearity (Belsley 1991). All condition indices in our model were

Table 1. Model covariates, descriptions, and summary statistics.

Variable name	Description	Landscape mean†	Bootstrap sample mean‡	Bootstrap sample SD‡
Response				
ΔNPV	change in non-photosynthetic vegetation fraction in pixel, i.e., wind damage (log-transformed)	0.034 (0.039)	0.1560 [0.1556, 0.1565]	0.1318 [0.1312, 0.1322]
Predictors				
Distance to edge	pixel distance to forest edge (m)	102.5 (2.5)	69.4 [68.0, 70.8]	2.39 [2.36, 2.44]
Secondary	binary variable for second growth§	0.53 (0.50)	0.59 [0.58, 0.60]	0.491 [0.490, 0.493]
Area	patch size in which pixel is located (ha)	33,247.5 (28,869.9)	33,035.4 [32,503.2, 33,605.0]	30,899.6 [30,592.6, 31,200.1]
Edginess (shape index)	shape index for patch in which pixel is located	24.4 (14.6)	24.9 [24.6, 25.2]	15.9 [15.7, 16.0]
Isolation (−1 × proximity index)	proximity index for patch in which pixel is located	75,887.7 (50,523.7)	−71,336.3 [−72,230.3, −70,415.9]	48,734.9 [47,999.9, 49,327.5]

† Mean with SD in parentheses.
‡ Mean with 95% bootstrapped CL in square brackets.
§ Binary; 0, old growth; 1, second growth.

<5. We tested for spatial autocorrelation among model residuals by calculating Moran's I and found no spatial autocorrelation in the model residuals (Moran's $I = 0.0003$, $P = 0.45$). Model parameters reported are the median estimates of the 200 bootstrapped models and 95% bootstrapped confidence intervals. Statistical analyses were conducted in R (R Core Team 2016).

Results

Overview: linking field and remote sensing data

Validation of ΔNPV with field observations.—Mean pre-damage AGB in field plots was 62.04 Mg C/ha (SD = 13.31, Appendix: Table S4). Mean AGB damaged was 17.5 Mg C/ha (SD = 18.7), or 24.6% of pre-storm AGB (SD = 25.1%). Mean stem density in field plots was 1,286 stems/ha (SD = 342.6), with an average 16.5% of stems damaged (SD = 15.7). Damaged stems were significantly larger than undamaged stems (Appendix: Fig. S5, $t = -9.73$, $P < 0.0001$).

ΔNPV was strongly related to damage as measured in the field plots. It was most strongly correlated with the proportion of stems damaged in field plots ($R^2 = 0.699$, Fig. 2), but the relationship held when damage was quantified in terms of total number of stems damaged ($R^2 = 0.649$), total AGB damaged ($R^2 = 0.542$), or proportion of AGB damaged ($R^2 = 0.603$, Appendix: Fig. S6). On average, ΔNPV was low across the landscape: mean ΔNPV was 0.03, and standard deviation was 0.04 (Fig. 4). Five percent of forest pixels, or 2,058 ha, had ΔNPV higher than 0.1, corresponding to 20.7% stems damaged, or 31.5% of carbon lost (22.5 Mg C/ha, Table 2). ΔNPV was >0.2 in 0.8% of forest pixels (348.5 ha), corresponding to 48.6% stems damaged, or 82.0% of carbon lost (59.1 Mg C/ha, Table 2). The total biomass lost as a result of the wind event in second-growth forests was 0.161 Tg C (95% CL = 0.026, 0.553, Table 2). When extrapolating across the whole study area, carbon lost was approximately 0.296 Tg C (95% CL = 0.05, 1.02), with 54% in second growth forest, and 46% in old growth (Table 2). Estimates for carbon lost in old-growth forest are based on extrapolation of data from second-growth forest, and therefore they are conservative estimates of total carbon lost.

Characterizing land cover and fragmentation.—The land cover classification accurately distinguished between oil palm, old-growth forest, second-growth forest, and other classes (Appendix: Table S3). Overall accuracy was 96.4%. Forty-four percent of the study area, 95,596 ha, was classified as forest. Forty percent of forest pixels were classified as old-growth forest and 60% were classified as second-growth forest (Fig. 1). There were 6,110 forest patches in the study area, with a mean area of 42.1 ha (Appendix: Fig. S7). Mean edginess (shape index) was 1.3, and mean isolation (−1 × proximity index) was −19,688 (Appendix: Fig. S7).

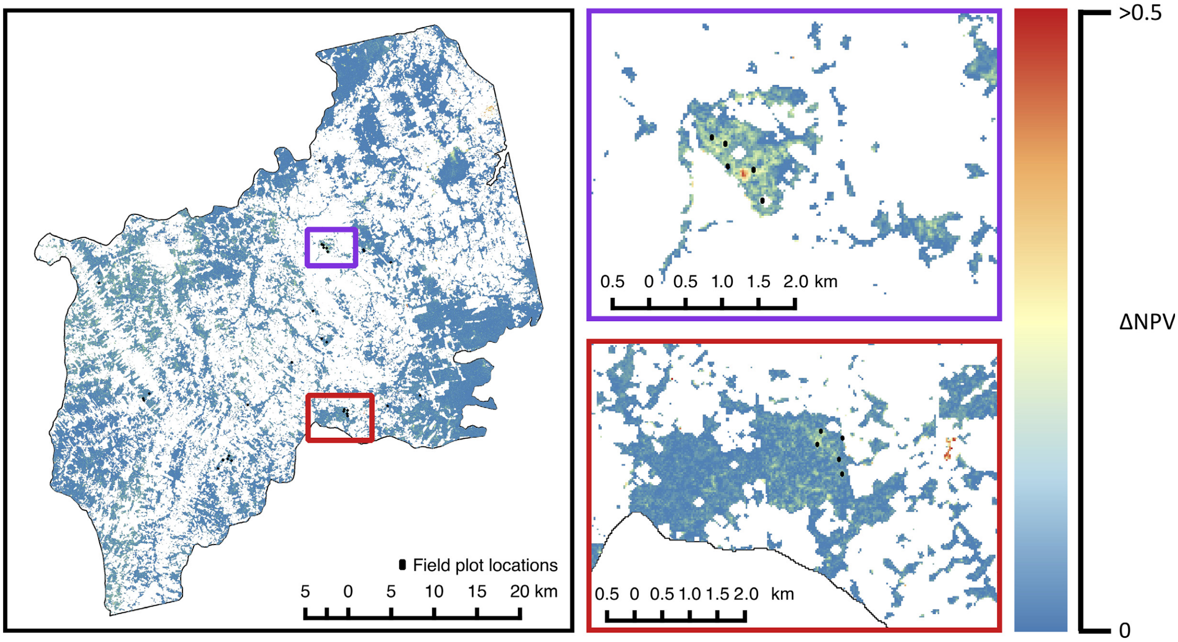

FIG. 4. Map of wind damage (ΔNPV) in study area. Insets show two areas of interest where several field plots were located.

Fragmentation in old- vs. second-growth forests

Degree of fragmentation varied across old-growth and second-growth forest pixels, with second-growth forests more fragmented along most measures (Fig. 5). Second-growth forest pixels were closer to forest edges (t = 237.15, P < 0.001, Appendix: Table S5), but in less edgy patches (t = 134.76, P < 0.0001, Appendix: Table S5). Second-growth pixels were also located in smaller (t = 141.28, P < 0.001, Fig. 5) and more isolated patches, (t = 47.658, P < 0.0001, Fig. 5).

Wind damage model

Fragmentation and forest type were significantly associated with ΔNPV (R^2 = 0.158, 95% bootstrap CL = [0.143, 0.173]). Distance to edge had the strongest association with ΔNPV (Fig. 6), which exponentially decreased with pixel distance from forest edge (Fig. 7a). Patch edginess was positively associated with ΔNPV, with pixels in edgier patches suffering more severe wind damage (Fig. 6, Fig. 7c). Isolation also influenced damage: ΔNPV was higher in more isolated patches (Figs. 6, 7d). Patch area was negatively associated with damage, though this effect was weaker than that of the other fragmentation predictors (Figs. 6, 7b). Predicted ΔNPV was slightly higher for old-growth forest pixels, though the difference between second growth and old growth was small compared to the predicted variation in ΔNPV associated with fragmentation (Figs. 6, 7).

DISCUSSION

Effects of fragmentation on wind damage

This study provides the first unequivocal empirical evidence that fragmentation increases risk of damage from extreme wind events in tropical forests. The severe convection event that occurred in our study region caused an overall loss of approximately 0.3 Tg C in the

TABLE 2. Summary of wind damage effects by forest type.

Parameter	Old growth	Second growth	All forest
Total area (ha)	38,137	57,459	95,596
Mean ΔNPV	0.033	0.035	0.034
Proportion pixels with ΔNPV >0.1	0.04	0.05	0.05
Proportion pixels with ΔNPV >0.2	0.01	0.01	0.01
Carbon lost (Tg C)	0.135 (0.020, 0.470)	0.161 (0.026, 0.553)	0.296 (0.05, 1.02)
Biomass lost per ha (Mg C/ha)	3.55 (0.519, 12.32)	2.79 (0.460, 9.63)	3.09

Note: 95% confidence intervals for lost carbon are in parentheses.

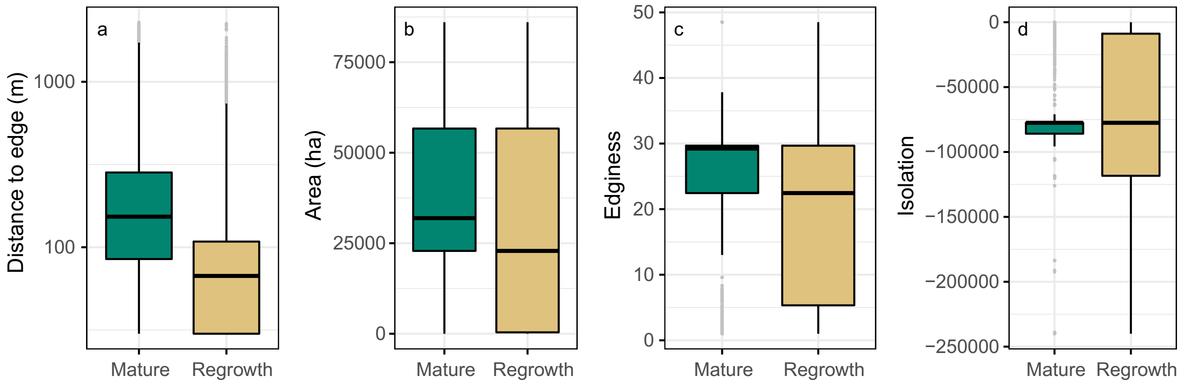

FIG. 5. Comparison of the distribution of fragmentation variables between old-growth and second-growth forest pixels. Boxes show 25%, 50%, and 75% quantiles and whisker endpoints are 2.5% and 97.5% quantiles of observed data. Light gray points are outliers. Figures include data from all forest pixels in the study area. Fragmentation variables are (a) distance to edge, (b) area, (c) edginess, and (d) isolation.

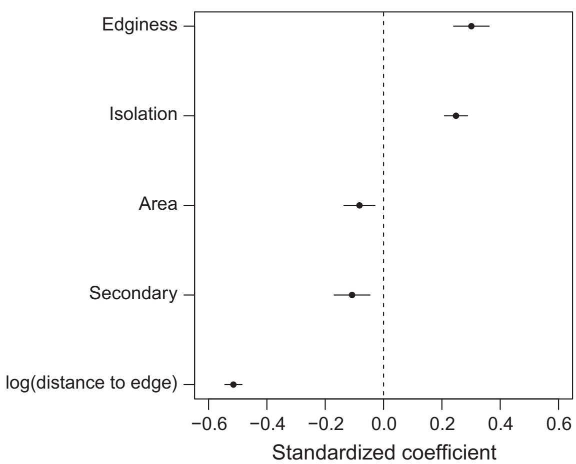

FIG. 6. Parameter estimates from wind damage model. Points show the median coefficient estimates from the 200 bootstrapped model fits, whiskers show bootstrapped 95% confidence interval.

study area (0.14 in second-growth forest and 0.16 in old-growth forest). When averaged across the total forested area in the study area (95,596 ha), this amounts to 3.09 Mg C/ha (2.79 Mg C/ha in second-growth, and 3.55 in old-growth), more than 60% greater per hectare than figures from a recent study that estimated annual carbon loss from natural disturbances in the entire Amazon forest (Espírito-Santo et al. 2014). That study estimated the total loss at 1.3 Pg C/yr, an average of 1.9 Mg C/ha across the ~6.8×10^8 ha of Amazon forest.

A number of differences between their study and ours could explain the discrepancy. The Espírito-Santo et al. study mapped disturbances across a study area many times the size of ours, and developed a disturbance size-frequency distribution for the entire Amazon. The disturbances captured in our far smaller study are likely on the intermediate-to-large end of their disturbance size-frequency distribution. However, the discrepancy might also reflect differences in landscape structure in the two studies. Espírito-Santo et al. focused on contiguous forest, where, based on our results, wind damage is likely to be less severe than in the fragmented landscapes of our study region. These findings illustrate the importance of considering fragmented landscapes when assessing disturbance regimes in tropical forests. Studies that do not consider the effects of landscape configuration may underestimate the importance of wind disturbance for quantifying the tropical forest carbon sink. Recent estimates suggest 70% of the world's forests are within 1 km of a forest edge (Haddad et al. 2015), and that 19% of tropical forests are <100 m from an edge (Brinck et al. 2017). Brinck et al. (2017) estimate that edge effects result in 0.34 Gt additional carbon emissions from tropical forests per year, though this estimate does not explicitly take into account effects of extreme winds. Considering the impacts of extreme winds in fragmented landscapes would likely affect estimates of the effects of fragmentation on forest carbon balance, and would influence our understanding of the importance of extreme wind events for driving carbon cycling in the Amazon.

Though many studies suggest that fragmented forests should have heightened vulnerability to wind damage (Saunders et al. 1991, Laurance and Curran 2008), evidence for this phenomenon has been lacking. For example, a number of studies that set out to measure effects of fragmentation on wind damage after Cyclone Larry, a category 5 tropical cyclone, found little difference in wind damage between fragments and continuous forest (Catterall et al. 2008, Grimbacher et al. 2008, Pohlman et al. 2008). Our study may have detected an effect where former studies did not for several reasons. First, the storm we considered was not as intense as a Cyclone Larry, and continuous forest cover may provide a protective benefit only up to a certain degree of storm intensity (Catterall et al. 2008). We do not have precise wind speed measurements from the date of the storm, but the

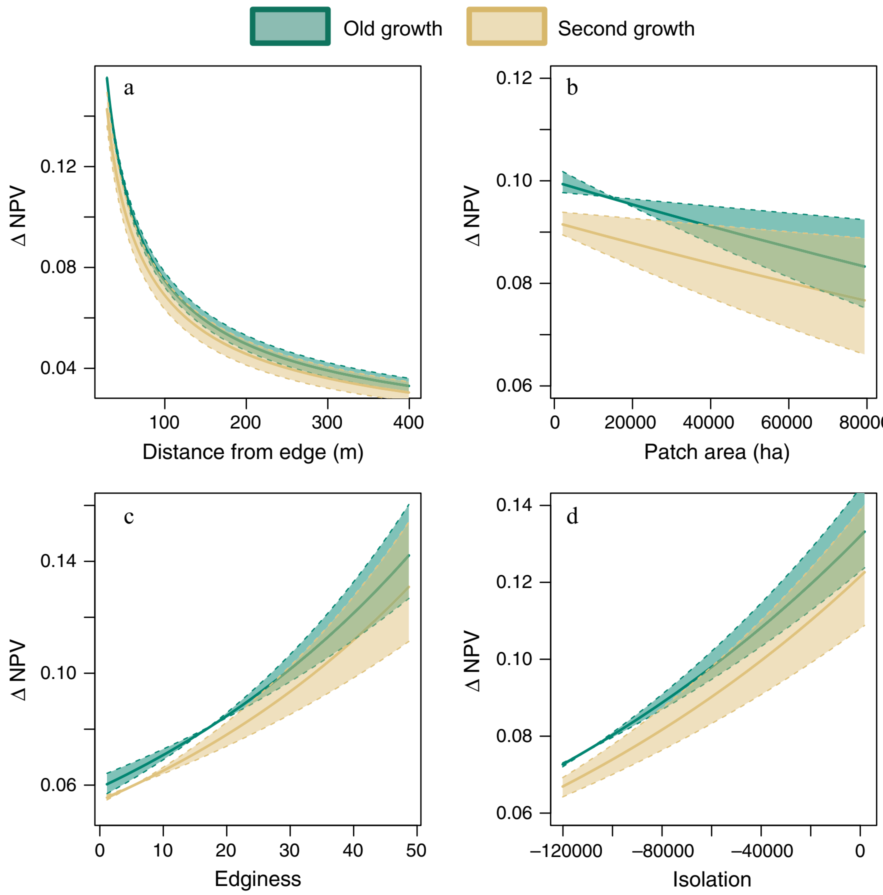

FIG. 7. Model predictions of ΔNPV and the fragmentation predictors. Solid lines depict predictions of the median coefficient estimates from bootstrapped model fits, dashed lines and shaded areas show predictions of 2.5% and 97.5% quantiles of coefficient estimates: (a) distance from edge, (b) patch area, (c) edginess (shape index), (d) isolation.

presence and intensity of overshooting tops indicates that winds were probably ≥93 km/h (Bedka and Khlopenkov 2016). In contrast, Category 5 tropical storms are associated with sustained winds >200 km/h. Lending support to this threshold hypothesis, a study after Hurricane Hugo in South Carolina found that in areas struck by the most intense part of the hurricane, species differences in wind resistance were not apparent (Hook et al. 1991). Differences in rates of damage across species were only observed in areas where wind speeds were lower. Variation in exposure and vulnerability to extreme winds due to species composition and landscape configuration may come into play only when winds are not so severe that they cause widespread damage regardless.

Second, previous studies of fragmentation and wind damage were based on field data from a relatively small number of plots. Heterogeneity in damage and wind speeds may have affected the statistical ability to detect underlying patterns related to fragmentation (Grimbacher et al. 2008). This patchiness and unmodeled variation in wind speeds is likely the reason for the substantial unexplained variance in our statistical models. However, because our remote sensing approach allows us to consider a broad landscape with a large sample size we are able to detect an effect of fragmentation despite the noise, demonstrating, as many other studies have, the usefulness of remote sensing for understanding ecosystems at landscape to regional scales (Chambers et al. 2007).

Fragmented forests may be more prone to wind damage via two main mechanisms: because they are exposed to stronger winds than continuous forest, or because they are more vulnerable to strong winds due to differences in species composition or forest structure (Laurance and Curran 2008). We found effects of all three axes of fragmentation—isolation, edge, and area—on wind damage, which suggests possible support for both mechanisms. The effects of isolation are probably due to exposure to stronger winds. Forest slows wind down; rougher surfaces exert more drag, leading to slower wind speeds (Davies-Colley et al. 2000). Wind picks up more speed over smoother vegetation types, like pasture. Because isolated fragments are surrounded by larger expanses of open areas and non-forest land cover types, they likely are subject to stronger winds. However, species composition may also differ depending on patch isolation. Because we do not have measurements of species composition in relation to isolation, we cannot rule out that differences in composition also contribute to the observed effect of isolation.

Edge and area effects on wind damage are more difficult to attribute to exposure vs. vulnerability, and could be due to either or both mechanisms. We found that pixels close to forest edges and pixels in edgier patches were more likely to be severely damaged. We also found a weak effect of patch size, likely because pixels in smaller patches are closer to edges. Forest edges are exposed to stronger winds (Somerville 1980, Morse et al. 2002), but there are also well-documented edge effects on species composition that could increase vulnerability to wind damage (Oosterhoorn and Kappelle 2000, Laurance et al. 2006). The degree to which differences in exposure or vulnerability explain the relationship between fragmentation and wind damage has implications for management actions to minimize impacts of strong winds. Future research could focus on disentangling the mechanisms responsible for these patterns.

Wind damage in old- vs. second-growth forest

The results from the model predicting wind damage (ΔNPV) indicate that when controlling for fragmentation, second-growth forests suffer slightly lower damage (have lower ΔNPV) than old-growth forests, counter to our initial hypothesis. Because trees with lower wood density are more prone to wind damage and community mean wood density tends to increase over succession in wet tropical forests (Bazzaz and Pickett 1980, Lohbeck et al. 2013), we hypothesized that wind damage would be more severe in second-growth forests. Our finding to the contrary may be due to differences in tree stature between old-growth and second-growth forests. Larger trees and more slender trees are more susceptible to wind damage, in particular to uprooting (Putz et al. 1983, Zimmerman et al. 1994, Everham and Brokaw 1996, Slodicak and Novak 2006, Canham et al. 2010, Ribeiro et al. 2016), which translates into differences in damage across sites with different forest structure. For example, Uriarte et al. (2004) found that damage after Hurricane Georges in the Dominican Republic was higher in sites with higher basal area and that young forests with low basal area were not severely affected by hurricane. Similarly, McGroddy et al. (2013) found that forest stands in the southern Yucatan with taller canopies and higher basal area suffered more severe hurricane damage, and that these structural differences were associated with past land use. Furthermore, because of the high levels of anthropogenic disturbance in the study area, we do not necessarily expect the successional shifts in species composition that are predicted for relatively undisturbed forests. Old-growth forests in the study area have never been completely cleared, but they have still been subject to anthropogenic disturbance, such as selective logging and fire. Selective logging tends to target timber species with higher wood density (Verburg and van Eijk-Bos 2003), so the largest remaining trees in selectively logged forests may be species with low wood density. Large stature and low-density wood would make these forest fragments especially prone to wind damage, perhaps explaining the higher damage we observed in old-growth forests. Alternatively, it is possible that large, high-wood-density trees are more vulnerable to wind, or that when they do fall, they result in larger blowdowns due to a domino effect of large, heavy trees causing more damage than trees with lighter wood. In future studies, additional field plot data, with information on forest stature, species identification and wood density from damaged vs. undamaged trees could help further elucidate which of these mechanisms drives the observed pattern.

In our model, however, fragmentation had a much stronger influence on damage than forest type (Figs. 6, 7). Second-growth forests in the study area are more fragmented than old-growth forests, which ultimately might result in more severe wind impacts in these forests. Elsewhere, studies have found that second growth tends to happen along forest margins and in small fragments surrounded by non-forest land use (Helmer 2000, Asner et al. 2009, Sloan et al. 2015). Wind is not the only disturbance for which risk is higher along edges: fire in the Amazon tends to be concentrated along forest edges (Cochrane and Laurance 2002, Alencar et al. 2004, Armenteras et al. 2013). There is potential for wind and fire to interact and amplify the other's impacts: studies in temperate ecosystems have found that an earlier fire can increase the severity of subsequent blow downs, and wind damage can increase the risk of fire by adding fuels and opening up the forest canopy (Myers and van Lear 1998, Kulakowski and Veblen 2002, 2007). These interactions might occur in the Amazon, and could exacerbate disturbance effects on forest carbon balance.

Wind and other disturbances can alter successional pathways in regrowing forests (Anderson-Teixeira et al. 2013, Uriarte et al. 2016). Variability in disturbance risk should thus be taken into account in spatial planning, management, and carbon accounting in tropical second-growth forests where the goal is to promote carbon sequestration. Silviculture has long considered wind damage risk in site and species selection and planting configuration (Somerville 1980, Savill 1983, Talkkari et al. 2000). However, managing tropical second-growth forests for carbon is a relatively new endeavor and the way landscape configuration influences susceptibility to disturbance is not well understood for tropical forests (U.S. Department of Energy 2012). However, where possible, and where risk of extreme winds is high, minimizing fragmentation and isolation could reduce risk of wind damage. Smallholders, too, get services such as timber or other forest products from forest fragments on their properties, and may wish to protect their forest fragments from the impacts of extreme winds. Promoting regrowth close to existing forests, maintaining less edgy patches, or planting wind-firm species in isolated fragments and close to forest edges are all steps that smallholders could take to reduce risk of wind damage in their forests.

Future research should attempt to disentangle the mechanisms behind the patterns observed in this study. Understanding the degree to which differences in vulnerability vs. exposure underlie variation in wind impacts will clarify appropriate management actions to minimize risk of wind damage in second-growth or remnant forests. Fragmentation experiments such as the Biological Dynamics of Forest Fragments experiment in Brazil have shed light on how fragmentation affects forest composition, structure, and microclimate (Laurance et al. 2002). However, understanding what those changes mean for impacts of extreme winds is not straightforward, and doing so would require some "luck" in that a severe windstorm would have to strike the experiment. This limitation presents some challenges in studying mechanisms of wind damage in fragmented landscapes, but there are ways forward. Fragmentation experiments like the aforementioned, but located in landscapes that suffer frequent severe wind events, such as Caribbean forests, could be useful in that the likelihood of extreme winds striking an experiment would be higher. However, an experimental approach relying on random chance is not the only way to further investigate these mechanisms. Improvements in modeling and mapping wind speed and in our understanding of how wind interacts with complex landscapes will further shed light on how exposure varies with fragmentation. Advances in remote sensing technology, which are beginning to provide a more detailed picture of forest structure and composition, will be useful in understanding ecological mechanisms responsible for variability in disturbance impacts (Chambers et al. 2007). Finally, much of what we already know about variation in species and stand susceptibility to wind comes from opportunistic field sampling after extreme winds (e.g., Zimmerman et al. 1994, Uriarte et al. 2004, McGroddy et al. 2013), and there is a need for further opportunistic post-storm sampling in fragmented landscapes. Continued monitoring of forest disturbance in fragmented landscapes, such as with the remote sensing approach demonstrated in this paper, is essential so that such opportunities are not lost. An improved understanding of how and why fragmentation and landscape configuration influence disturbance regimes in tropical second-growth forests will help ensure that the carbon potential of tropical second-growth forests is better achieved.

Acknowledgments

We thank C. Gabriel Hidalgo, Luís Calderon Vasquez, Robert Piña, and Geancarlo Cohello for assistance with fieldwork. Thanks to the Uriarte and DeFries lab groups, and Bianca Lopez for helpful feedback on early drafts of this manuscript. We acknowledge support from the Institute for Latin American Studies at Columbia University, and the Center for International Forestry Research (CIFOR).

Literature Cited

Adams, J. B., and A. R. Gillespie. 2006. Remote sensing of landscapes with spectral images. Cambridge University Press, Cambridge, UK.

Alencar, A. A. C., L. A. Solorzano, and D. C. Nepstad. 2004. Modeling forest understory fires in an eastern Amazonian landscape. Ecological Applications 14:139–149.

Anderson-Teixeira, K. J., A. D. Miller, J. E. Mohan, T. W. Hudiburg, B. D. Duval, and E. H. DeLucia. 2013. Altered dynamics of forest recovery under a changing climate. Global Change Biology 19:2001–2021.

Armenteras, D., T. M. González, and J. Retana. 2013. Forest fragmentation and edge influence on fire occurrence and intensity under different management types in Amazon forests. Biological Conservation 159:73–79.

Asner, G. P., T. K. Rudel, T. M. Aide, R. DeFries, and R. Emerson. 2009. A contemporary assessment of change in humid tropical forests. Conservation Biology 23:1386–1395.

Bazzaz, F. A., and S. Pickett. 1980. Physiological ecology of tropical succession: a comparative review. Annual Review of Ecology and Systematics 11:287–310.

Bedka, K. M., and K. Khlopenkov. 2016. A probabilistic multispectral pattern recognition method for detection of overshooting cloud tops using passive satellite imager observations. Journal of Applied Meteorology and Climatology 55:1983–2005, *in press*.

Bellingham, P. J., V. Kapos, and N. Varty. 1992. Hurricanes need not cause high mortality: the effects of Hurricane Gilbert on forests in Jamaica. Journal of Tropical Ecology 8:217–223.

Belsley, D. A. 1991. A guide to using the collinearity diagnostics. Computer Science in Economics and Management 4:33–50.

Boardman, J. W., F. A. Kruse, and R. O. Green. 1995. Mapping target signatures via partial unmixing of AVIRIS data. Pages 23–26 *in* Proceedings of the Fifth JPL Airborne Earth Science Workshop. JPL Publication, Volume 95-01. Jet Propulsion Laboratory, Pasadena, California, USA.

Brinck, K., R. Fischer, J. Groeneveld, S. Lehmann, M. Dantas De Paula, S. Pütz, J. O. Sexton, D. Song, and A. Huth. 2017. High resolution analysis of tropical forest fragmentation and its impact on the global carbon cycle. Nature Communications 8:14855.

Brown, S., and A. E. Lugo. 1982. The storage and production of organic matter in tropical forests and their role in the global carbon cycle. Biotropica 14:161–187.

Brown, S., and A. E. Lugo. 1990. Tropical secondary forests. Journal of Tropical Ecology 6:1–32.

Canham, C. D., J. Thompson, J. K. Zimmerman, and M. Uriarte. 2010. Variation in susceptibility to hurricane damage as a function of storm intensity in Puerto Rican tree species. Biotropica 42:87–94.

Canty, M. J., and A. A. Nielsen. 2008. Automatic radiometric normalization of multitemporal satellite imagery with the iteratively re-weighted MAD transformation. Remote Sensing of Environment 112:1025–1036.

Catterall, C. P., S. McKenna, J. Kanowski, and S. D. Piper. 2008. Do cyclones and forest fragmentation have synergistic effects? A before–after study of rainforest vegetation structure at multiple sites. Austral Ecology 33:471–484.

Chambers, J. Q., G. P. Asner, D. C. Morton, L. O. Anderson, S. S. Saatchi, F. D. B. Espírito-Santo, M. Palace and C. Souza. 2007. Regional ecosystem structure and function: ecological insights from remote sensing of tropical forests. Trends in Ecology & Evolution 22:414–423.

Chambers, J. Q., R. I. Negrón-Juárez, G. C. Hurtt, D. M. Marra, and N. Higuchi. 2009. Lack of intermediate-scale disturbance data prevents robust extrapolation of plot-level tree mortality rates for old-growth tropical forests. Ecology Letters 12:E22–E25.

Chambers, J. Q., R. I. Negrón-Juárez, D. M. Marra, et al. 2013. The steady-state mosaic of disturbance and succession across an old-growth Central Amazon forest landscape. Proceedings of the National Academy of Sciences USA 110:3949–3954.

Chazdon, R. L., et al. 2016. Carbon sequestration potential of second-growth forest regeneration in the Latin American tropics. Science Advances 2:e1501639.

Cochrane, M. A., and W. F. Laurance. 2002. Fire as a large-scale edge effect in Amazonian forests. Journal of Tropical Ecology 18:311–325.

Curran, T. J., R. L. Brown, E. Edwards, et al. 2008. Plant functional traits explain interspecific differences in immediate cyclone damage to trees of an endangered rainforest community in north Queensland. Austral Ecology 33:451–461.

Davies-Colley, R. J., G. W. Payne, and M. Van Elswijk. 2000. Microclimate gradients across a forest edge. New Zealand Journal of Ecology 24:111–121.

de Casaneve, J. L., J. P. Pelotto, and J. Protomastro. 1995. Edge-interior differences in vegetation structure and composition in a Chaco Semiarid Forest, Argentina. Forest Ecology and Management 72:61–69.

Del Genio, A. D., M.-S. Yao, and J. Jonas. 2007. Will moist convection be stronger in a warmer climate? Geophysical Research Letters 34:L16703.

Di Vittorio, A. V., R. I. Negrón-Juárez, N. Higuchi, and J. Q. Chambers. 2014. Tropical forest carbon balance: effects of field- and satellite-based mortality regimes on the dynamics and the spatial structure of Central Amazon forest biomass. Environmental Research Letters 9:034010.

Dormann, C. F., J. Elith, S. Bacher, et al. 2012. Collinearity: a review of methods to deal with it and a simulation study evaluating their performance. Ecography 36:27–46.

Dworak, R., K. M. Bedka, J. Brunner, and W. Feltz. 2012. Comparison between GOES-12 overshooting top detections, WSR-88D radar reflectivity, and severe storm reports. Weather and Forecasting 10:1811–1822.

Espírito-Santo, F. D. B., M. Gloor, M. Keller, et al. 2014. Size and frequency of natural forest disturbances and the Amazon forest carbon balance. Nature Communications 5:3434.

Espírito-Santo, F. D. B., M. Keller, B. Braswell, B. W. Nelson, S. Frolking, and G. Vicente. 2010. Storm intensity and old-growth forest disturbances in the Amazon region. Geophysical Research Letters 37:L11403.

Everham, E. M., and N. V. Brokaw. 1996. Forest damage and recovery from catastrophic wind. Botanical Review 62:113–185.

Fahrig, L. 2003. Effects of habitat fragmentation on biodiversity. Annual Review of Ecology, Evolution, and Systematics 34:487–515.

Ferreira, L. V., and W. F. Laurance. 1997. Effects of forest fragmentation on mortality and damage of selected trees in central Amazonia. Conservation Biology 11:797–801.

Fisher, J. I., G. C. Hurtt, R. Q. Thomas, and J. Q. Chambers. 2008. Clustered disturbances lead to bias in large-scale estimates based on forest sample plots. Ecology Letters 11: 554–563.

Flynn, D. F. B., M. Uriarte, T. Crk, J. B. Pascarella, J. K. Zimmerman, T. M. Aide, and M. A. Caraballo Ortiz. 2009. Hurricane disturbance alters secondary forest recovery in Puerto Rico. Biotropica 42:149–157.

Fons, W. L. 1940. Influence of forest cover on wind velocity. Journal of Forestry 38:481–486.

Fox, J., and G. Monette. 1992. Generalized collinearity diagnostics. Journal of the American Statistical Association 87:178–183.

Garstang, M., H. L. Massie, J. Halverson, S. Greco, and J. Scala. 1994. Amazon coastal squall lines. 1. Structure and kinematics. Monthly Weather Review 122:608–622.

Garstang, M., S. White, H. H. Shugart, and J. Halverson. 1998. Convective cloud downdrafts as the cause of large blowdowns in the Amazon rainforest. Meteorology and Atmospheric Physics 67:199–212.

Gelman, A., and J. Hill. 2007. Data analysis using regression and multilevelhierarchical models. Volume 1. Cambridge University Press, New York, New York, USA.

Graham, M. H. 2003. Confronting multicollinearity in ecological multiple regression. Ecology 84:2809–2815.

Grimbacher, P. S., C. P. Catterall, and N. E. Stork. 2008. Do edge effects increase the susceptibility of rainforest fragments to structural damage resulting from a severe tropical cyclone? Austral Ecology 33:525–531.

Grove, S. J., S. M. Turton, and D. T. Siegenthaler. 2000. Mosaics of canopy openness induced by tropical cyclones in lowland rain forests with contrasting management histories in northeastern Australia. Journal of Tropical Ecology 16: 883–894.

Gutiérrez-Vélez, V. H., and R. DeFries. 2013. Annual multi-resolution detection of land cover conversion to oil palm in the Peruvian Amazon. Remote Sensing of Environment 129: 154–167.

Gutiérrez-Vélez, V. H., R. DeFries, M. Pinedo-Vasquez, et al. 2011. High-yield oil palm expansion spares land at the expense of forests in the Peruvian Amazon. Environmental Research Letters 6:044029.

Haddad, N. M., L. A. Brudvig, J. Clobert, et al. 2015. Habitat fragmentation and its lasting impact on earth's ecosystems. Science Advances 1:e1500052.

Hall, F. G., D. E. Strebel, J. E. Nickeson, and S. J. Goetz. 1991. Radiometric rectification: toward a common radiometric response among multidate, multisensor images. Remote Sensing of Environment 35(1):11–27.

Harper, K. A., S. E. Macdonald, P. J. Burton, et al. 2005. Edge influence on forest structure and composition in fragmented landscapes. Conservation Biology 19:768–782.

Helmer, E. H. 2000. The landscape ecology of tropical secondary forest in Montane Costa Rica. Ecosystems 3:98–114.

Hook, D. D., M. A. Buford, and T. M. Williams. 1991. Impact of Hurricane Hugo on the South Carolina coastal plain forest. Journal of Coastal Research 8:291–300.

Imbert, D., P. Labbe, and A. Rousteau. 1996. Hurricane damage and forest structure in Guadeloupe, French West Indies. Journal of Tropical Ecology 12:663–680.

IPCC. 2013. Climate change 2013: the physical science basis. Pages 1535 *in* T. F. Stocker, D. Qin, G.-K. Plattner, M. Tignor, S. K. Allen, J. Boschung, A. Nauels, Y. Xia, V. Bex, and P. M. Midgley, editors. Contribution of Working Group I to the Fifth Assessment Report of the Intergovern- mental Panel on Climate Change. Cambridge University Press, Cambridge, UK; New York, New York, USA.

Jakovac, C. C., F. Bongers, T. W. Kuyper, R. C. Mesquita, and M. Peña-Claros. 2016. Land use as a filter for species composition in Amazonian secondary forests. Journal of Vegetation Science 27:1104–1116.

Kanowski, J., C. P. Catterall, S. G. McKenna, and R. Jensen. 2008. Impacts of cyclone Larry on the vegetation structure of timber plantations, restoration plantings and rainforest on the Atherton Tableland, Australia. Austral Ecology 33: 485–494.

Knutson, T. R., J. L. McBbride, J. Chan, et al. 2010. Tropical cyclones and climate change. Nature Geoscience 3:157–163.

Kulakowski, D., and T. T. Veblen. 2002. Influences of fire history and topography on the pattern of a severe wind blowdown in a Colorado subalpine forest. Journal of Ecology 90:806–819.

Kulakowski, D., and T. T. Veblen. 2007. Effect of prior disturbances on the extent and severity of wildfire in Colorado subalpine forests. Ecology 88:759–769.

Laurance, W. F., and T. J. Curran. 2008. Impacts of wind disturbance on fragmented tropical forests: a review and synthesis. Austral Ecology 33:399–408.

Laurance, W. F., S. G. Laurance, L. V. Ferreira, J. M. Rankin-de Merona, C. Gascon, and T. E. Lovejoy. 1997. Biomass collapse in Amazonian forest fragments. Science 278:1117–1118.

Laurance, W. F., T. E. Lovejoy, H. L. Vasconcelos, et al. 2002. Ecosystem decay of Amazonian forest fragments: a 22-year investigation. Conservation Biology 16:605–618.

Laurance, W. F., H. E. M. Nascimento, S. G. Laurance, A. C. Andrade, P. M. Fearnside, J. E. L. Ribeiro, and R. L. Capretz. 2006. Rain forest fragmentation and the proliferation of successional trees. Ecology 87:469–482.

Loehle, C. 1991. Managing and monitoring ecosystems in the face of heterogeneity. Pages 144–159 *in* J. Kolasa and S. T. A. Pickett, editors. Ecological heterogeneity. Springer-Verlag, New York, New York, USA.

Lohbeck, M., L. Poorter, E. Lebrija-Trejos, et al. 2013. Successional changes in functional composition contrast for dry and wet tropical forest. Ecology 94:1211–1216.

Lugo, A. E. 2008. Visible and invisible effects of hurricanes on forest ecosystems: an international review. Austral Ecology 33:368–398.

Magnabosco Marra, D., et al. 2016. Predicting biomass of hyperdiverse and structurally complex central Amazonian forests – A virtual approach using extensive field data. Biogeosciences 13:1553–1570.

McGarigal, K., S. A. Cushman, M. C. Neel and E. Ene. 2012. FRAGSTATS v4: spatial pattern analysis program for categorical and continuous maps. University of Massachusettes, Amherst, Massachusetts, USA. http://www.umass.edu/landeco/research/fragstats/fragstats.html

McGroddy, M., D. Lawrence, L. Schneider, J. Rogan, I. Zager, and B. Schmook. 2013. Damage patterns after Hurricane Dean in the southern Yucatán: Has human activity resulted in more resilient forests? Forest Ecology and Management 310:812–820.

Mesquita, R., P. Delamônica, and W. F. Laurance. 1999. Effect of surrounding vegetation on edge-related tree mortality in Amazonian forest fragments. Biological Conservation 91: 129–134.

Mitchell, S. J. 2012. Wind as a natural disturbance agent in forests: a synthesis. Forestry 86:147–157.

Morse, A. P., B. A. Gardiner, and B. J. Marshall. 2002. Mechanisms controlling turbulence development across a forest edge. Boundary-Layer Meteorology 103:227–251.

Myers, R. K., and D. H. van Lear. 1998. Hurricane–fire interactions in coastal forests of the south: a review and hypothesis. Forest Ecology and Management 103:265–276.

Negrón-Juárez, R. I., J. Q. Chambers, G. Guimaraes, et al. 2010. Widespread Amazon forest tree mortality from a single cross-basin squall line event. Geophysical Research Letters 37:L16701.

Negrón-Juárez, R. I., J. Q. Chambers, D. M. Marra, G. H. P. M. Ribeiro, S. W. Rifai, N. Higuchi, and D. Roberts. 2011. Detection of subpixel treefall gaps with Landsat imagery in Central Amazon. Remote Sensing of Environment 115:3322–3328.

Nelson, B. W., R. Mesquita, J. L. G. Pereira, S. G. A. Souza, G. T. Batista and L. B. Couto. 1999. Allometric regressions for improved of secondary forest biomass in the central Amazon. Forest Ecology and Management 117:149–167.

Nelson, B. W., V. Kapos, J. B. Adams, W. J. Oliveira, and O. P. Braun. 1994. Forest disturbance by large blowdowns in the Brazilian Amazon. Ecology 75:853–858.

Oliveira, P. J. C., G. P. Asner, D. E. Knapp, et al. 2007. Land-use allocation protects the Peruvian Amazon. Science 317: 1233–1236.

Oliver, H. R. 1971. Wind profiles in and above a forest canopy. Quarterly Journal of the Royal Meteorological Society 97:548–553.

Oosterhoorn, M., and M. Kappelle. 2000. Vegetation structure and composition along an interior-edge-exterior gradient in a Costa Rican montane cloud forest. Forest Ecology and Management 126:291–307.

Orlowsky, B., and S. I. Seneviratne. 2012. Global changes in extreme events: regional and seasonal dimension. Climatic Change 110:669–696.

Peltola, H. 1996. Model computations on wind flow and turning moment by wind for Scots pines along the margins of clear-cut areas. Forest Ecology and Management 83:203–215.

Pohlman, C. L., M. Goosem, and S. M. Turton. 2008. Effects of Severe Tropical Cyclone Larry on rainforest vegetation and understorey microclimate near a road, powerline and stream. Austral Ecology 33:503–515.

Poorter, L., F. Bongers, T. M. Aide, et al. 2016. Biomass resilience of neotropical secondary forests. Nature 530:211–214.

Putz, F. E., P. D. Coley, K. Lu, A. Montalvo, and A. Aiello. 1983. Uprooting and snapping of trees: structural determinants and ecological consequences. Canadian Journal of Forest Research 13:1011–1020.

Quine, C. P., and B. A. Gardiner. 2007. Understanding how the interaction of wind and trees results in windthrow, stem breakage, and canopy gap formation. Pages 103–156 *in* E. A. Johnson and K. Miyanishi, editors. Plant disturbance ecology: the process and the response. Elsevier, Burlington, Massachusetts, USA.

Ramos da Silva, R., D. Werth, and R. Avissar. 2008. Regional impacts of future land-cover changes on the Amazon Basin wet-season climate. Journal of Climate 21:1153–1170.

Ribeiro, G. H. P. M., et al. 2016. Mechanical vulnerability and resistance to snapping and uprooting for Central Amazon tree species. Forest Ecology and Management 380:1–10.

Rifai, S. W., J. D. Urquiza Muñoz, R. I. Negrón-Juárez, et al. 2016. Landscape-scale consequences of differential tree mortality from catastrophic wind disturbance in the Amazon. Ecological Applications 26:2225–2237.

Saunders, D. A., R. J. Hobbs, and C. R. Margules. 1991. Biological consequences of ecosystem fragmentation—a review. Conservation Biology 5:18–32.

Savill, P. S. 1983. Silviculture in windy climates. Forestry Abstracts 44:473–488.

Schwartz, N. B., M. Uriarte, R. DeFries, V. H. Gutierrez-Velez, and M. A. Pinedo-Vasquez. *In press.* Land-use dynamics influence estimates of carbon sequestration potential in tropical second-growth forest. Environmental Research Letters. DOI: https://doi.org/10.1088/1748-9326/aa708b

Schwartz, N. B., M. Uriarte, V. H. Gutierrez-Velez, W. Baethgen, R. DeFries, K. Fernandes, and M. A. Pinedo-Vasquez. 2015. Climate, landowner residency, and land cover predict local scale fire activity in the Western Amazon. Global Environmental Change 31:144–153.

Sloan, S., M. Goosem, and S. G. Laurance. 2015. Tropical forest regeneration following land abandonment is driven by primary rainforest distribution in an old pastoral region. Landscape Ecology 31:601–618.

Slodicak, M., and J. Novak. 2006. Silvicultural measures to increase the mechanical stability of pure secondary Norway spruce stands before conversion. Forest Ecology and Management 224:252–257.

Somerville, A. 1980. Wind stability—forest layout and silviculture. New Zealand Journal of Forestry Science 10:476–501.

Talkkari, A., H. Peltola, S. Kellomäki, and H. Strandman. 2000. Integration of component models from the tree, stand and regional levels to assess the risk of wind damage at forest margins. Forest Ecology and Management 135:303–313.

Uriarte, M., C. D. Canham, J. Thompson, and J. K. Zimmerman. 2009. Understanding natural disturbance and human land use as determinants of tree community dynamics in a subtropical wet forest: Results from a forest simulator. Ecological Monographs 79:423–443.

Uriarte, M., J. S. Clark, J. K. Zimmerman, L. S. Comita, J. Forero-Montaña, and J. Thompson. 2012. Multidimensional trade-offs in species responses to disturbance: implications for diversity in a subtropical forest. Ecology 93: 191–205.

Uriarte, M., L. W. Rivera, J. K. Zimmerman, T. M. Aide, A. G. Power, and A. S. Flecker. 2004. Effects of land use history on hurricane damage and recovery in a neotropical forest. Plant Ecology 174:49–58.

Uriarte, M., N. Schwartz, J. S. Powers, E. Marin-Spiotta, W. Liao, and L. K. Werden. 2016. Impacts of climate variability on tree demography in second growth tropical forests: the importance of regional context for predicting successional trajectories. Biotropica 48:780–797.

U.S. Department of Energy. 2012. Research Priorities for Tropical Ecosystems Under Climate Change Workshop Report, DOE/SC-0153. Pages 134. U.S. Department of Energy Office of Science. science.energy.gov/ber/news-and-resources/

USGS. 2016. Product guide: Provisional Landsat 8 Surface Reflectance Code (LaSRC) product. http://landsat.usgs.gov/documents/provisional_lasrc_product_guide.pdf

Verburg, R., and C. van Eijk-Bos. 2003. Effects of selective logging on tree diversity, composition and plant functional type patterns in a Bornean rain forest. Journal of Vegetation Science 14:99–110.

Zeng, H., H. Peltola, A. Talkkari, A. Venäläinen, H. Strandman, S. Kellomäki, and K. Wang. 2004. Influence of clearcutting on the risk of wind damage at forest edges. Forest Ecology and Management 203:77–88.

Zhu, Z., and C. E. Woodcock. 2012. Object-based cloud and cloud shadow detection in Landsat imagery. Remote Sensing of Environment 118:83–94.

Zimmerman, J. K., E. M. Everham III, R. B. Waide, D. J. Lodge, C. M. Taylor, and N. V. Brokaw. 1994. Responses of tree species to hurricane winds in subtropical wet forest in Puerto Rico: implications for tropical tree life histories. Journal of Ecology 82:911–922.

Supporting Information

Additional supporting information may be found online at: http://onlinelibrary.wiley.com/doi/10.1002/eap.1576/full

Data Availability

Data available from the Columbia Academic Commons: https://doi.org/10.7916/d8vh5v6w